

This is a postprint version of the following published document:

Jiménez-Ubieto, A., Poza, M., Martín-Muñoz, A. et al.
Real-life disease monitoring in follicular lymphoma
patients using liquid biopsy ultra-deep sequencing and
PET/CT. *Leukemia* 37, 659–669 (2023). [https://
doi.org/10.1038/s41375-022-01803-x](https://doi.org/10.1038/s41375-022-01803-x)

DOI: [10.1038/s41375-022-01803-x](https://doi.org/10.1038/s41375-022-01803-x)

© 2023, The Author(s), under exclusive licence to Springer Nature
Limited

1 **Real-Life Disease Monitoring in Follicular Lymphoma Patients Using Liquid Biopsy Ultra-Deep**
2 **Sequencing and PET/CT**

3
4 Ana Jiménez-Ubieto^{1*}, María Poza^{1*}, Alejandro Martin-Muñoz², Yanira Ruiz-Heredia^{1,2}, Sara
5 Dorado^{2,3}, Gloria Figaredo⁴, Juan Manuel Rosa-Rosa¹, Antonia Rodriguez¹, Carmen Barcena⁵,
6 Laura Parrilla Navamuel⁴, Jaime Carrillo², Ricardo Sanchez^{1,2}, Laura Rufian^{1,2}, Alexandra
7 Juárez^{1,2}, Margarita Rodriguez^{1,2}, Chongwu Wang⁶, Paula de Toledo³, Carlos Grande⁷, Manuela
8 Mollejo⁴, Luis-Felipe Casado⁴, María Calbacho¹, Tycho Baumann¹, Inmaculada Rapado¹, Miguel
9 Gallardo^{1,8}, Pilar Sarandeses⁹, Rosa Ayala¹, Joaquín Martínez-López^{1*}, Santiago Barrio^{1,2*}

10
11 ¹Department of Hematology, Hospital Universitario 12 de Octubre, Instituto de Investigación
12 Sanitaria Hospital 12 de Octubre (imas12), CNIO, CIBERONC, Madrid, Spain.

13 ²Altum sequencing Co., Madrid, Spain.

14 ³Computational Science Department, Carlos III University, Madrid, Spain.

15 ⁴Hospital General Universitario de Toledo, Toledo, Spain.

16 ⁵Hospital Universitario 12 de Octubre, Departamento de Anatomía Patológica, Madrid, Spain.

17 ⁶Hosea Precision Medical Technology Co., Ltd., Weihai, Shangdong, China.

18 ⁷Clínica Universitaria de Navarra, Madrid, Spain.

19 ⁸H120-CNIO Haematological Malignancies Clinical Research Unit, CNIO, Madrid, Spain.

20 ⁹Hospital Universitario 12 de Octubre, Departamento de Medicina Nuclear, Madrid, Spain.

21
22 *These authors contributed equally to this work.

23
24 **Running Title:** Liquid biopsy minimal residual disease monitoring in follicular lymphoma

26 **Keypoint:** Liquid Biopsy MRD quantification in follicular lymphoma in combination with PET/CT
27 identifies POD24 patients with 89% sensitivity and 100% specificity

28

29 **Keywords:** Follicular Lymphoma, Liquid Biopsy, PET/CT, Minimal Residual Disease, cfDNA

30

31

32

33 **Correspondence**

34 Ana Jiménez Ubieto and Santiago Barrio

35 Hematology Department

36 Doce de Octubre University

37 Hospital Avenida de Córdoba s/n.

38 28041, Madrid

39 Spain

40 Emails: anitiju@hotmail.com, santibarrio0.3@gmail.com

41

42

43

44

45

46

47

48

49

50

51 **Abstract**

52
53 In the present study, we screened 84 Follicular Lymphoma patients for somatic mutations suitable as liquid
54 biopsy MRD biomarkers using a targeted next-generation sequencing (NGS) panel. We found trackable
55 mutations in 95% of the lymph node samples and 80% of the liquid biopsy baseline samples. Then, we
56 used an ultra-deep sequencing approach with $2 \cdot 10^{-4}$ sensitivity (LiqBio-MRD) to track those mutations
57 on 151 follow-up liquid biopsy samples from 54 treated patients. Positive LiqBio-MRD at first-line therapy
58 correlated with a higher risk of progression both at the interim evaluation (HR_{INT} 11.0, 95% CI 2.10–57.7, p
59 = 0.005) and at the end of treatment (HR_{EOT} , HR 19.1, 95% CI 4.10–89.4, $p < 0.001$). Similar results were
60 observed by PET/CT Deauville score, with a median PFS of 19 months vs. NR ($p < 0.001$) at the interim and
61 13 months vs. NR ($p < 0.001$) at EOT. LiqBio-MRD and PET/CT combined identified the patients that
62 progressed in less than two years with 88% sensitivity and 100% specificity. Our results demonstrate that
63 LiqBio-MRD is a robust and non-invasive approach, complementary to metabolic imaging, for identifying
64 FL patients at high risk of failure during the treatment and should be considered in future response-
65 adapted clinical trials.

66
67 **Introduction**

68
69 Follicular lymphoma (FL) is the second most common non-Hodgkin lymphoma in developed countries (1).
70 It is genetically characterized by an upregulation of BCL2 in the progenitor B cell that transforms into a
71 proliferating clone driven by t(14;18) translocations(2). Nowadays, FL is considered an indolent disorder
72 with a relatively favorable course. Long remissions are often achieved with modern day treatments, with
73 median survival rates approaching 20 years (3,4). However, 15–20% of patients are primary refractory or
74 progress during the first two years after first-line therapy (POD24). These patients present a poor outcome,
75 with 5-year overall survival (OS) probabilities between 38% and 50% (5,6).

76

77 The disease is characterized by a remitting, relapsing clinical course with progressive shortening of
78 response duration after treatment. Moreover, high-grade transformation (HT) to aggressive lymphoma
79 occurs in around 3% of the patients per year (7–10). Global research efforts have been aimed at identifying
80 patients with a high risk of progression and transformation to optimize the duration of treatment response
81 and to ease suffering and morbidity. Many clinical, molecular, pathological, and imaging biomarkers have
82 been described and used to stratify/group FL patients into several risk categories at diagnosis (11–19).
83 However, most of these tools remain inaccessible in daily practice and have not been adequately tested
84 to select the best therapy.

85

86 For this reason, as the understanding of prognosis is crucial, the ultimate goal in a disease such as FL should
87 be to develop tools and approaches to guide therapy. Current studies of risk-adapted therapy based on
88 minimal residual disease (MRD) evaluation remain to be investigational in FL (20). At the molecular level,
89 several studies have shown that MRD assessment is predictive of outcome. Most of these studies have
90 focused on evaluating the BCL2/IgH rearrangements, quantified by polymerase chain reaction (PCR) in
91 bone marrow or peripheral blood. The levels of circulating cell-free DNA (cfDNA) fragments have also
92 demonstrated predictive value (21,22). However, unlike in diffuse large B cell lymphoma (DLBCL), in FL,
93 there are no studies evaluating MRD based on tumoral cfDNA detection (23,24).

94

95 In contrast, PET/CT using the 5-point scale Deauville criteria (D5PS) is well established, regardless of the
96 treatment used (25,26), to predict the outcome and attain complete metabolic response. Nevertheless,
97 the use of PET/CT alone is hampered by its limited sensitivity and specificity, and the interpretation of the
98 results is highly dependent on the evaluating radiologist (27,28). Moreover, there is little information on
99 interim PET/CT (26) and its combination with MRD for prognostic assessment (20,29), and there are no
100 studies that have used liquid biopsy NGS methods. Therefore, in this study, we aim to analyze the response

101 to therapy in FL patients using ultra-deep sequencing of cfDNA and the D5PS scale PET/CT to identify, early
102 on, those patients who have a high risk of relapse in less than 24 months (POD24).

103

104 **Materials/Subjects and Methods**

105

106 *Patient Cohort and Study Design*

107

108 This study was designed as a prospective observational study. The cohort included 84 newly diagnosed,
109 recurrent or transformed FL patients recruited from the routine clinical practice at the Hospital 12 de
110 Octubre (H12O) in Madrid, Spain, and the Hospital Universitario de Toledo, Spain. Of the initial 84 patients,
111 58 were under first-line treatment, 15 received salvage therapy and 11 did not receive treatment
112 (Supplemental figure S1). The median follow-up for the patients in first-line therapy was 20.5 months (rank
113 3-65.5), and 31 (rank 5-43.5) months for patients in salvage treatment. One patient (FL5), suffered from a
114 transformation 10 months after the first-line therapy started. After transformation, the patient was
115 included as a transformed case (FL5t). Informed written consent of all patients was obtained according to
116 the Declaration of Helsinki. The study inclusion criteria were; histological confirmation and the availability
117 of enough biological material in sequential samples. Treatment was started according to the *Groupe*
118 *d'Etude des Lymphomes Folliculaires* criteria (30), and imaging examinations were performed as ordinary
119 clinical practice. Responsible physicians decided on the treatment regimen according to institutional and
120 international guidelines. In all patients, DNA from lymph node biopsies and cfDNA was obtained before
121 the treatment was started. Somatic mutations of these samples were selected as disease biomarkers for
122 liquid biopsy MRD (LiqBio-MRD) analysis at follow-up time-points. The following biological materials were
123 analyzed: DNA from formalin-fixed paraffin-embedded (FFPE) lymph node biopsies ($n = 75$) and cfDNA (n
124 $= 44$) before treatment start, and follow-up cfDNA samples during chemo-immunotherapy courses ($n =$
125 151).

126
127 *DNA extraction*
128
129 Lymph node DNA was extracted with a Qiamp gDNA FFPE kit (Qiagen, Hilden, Germany) using two to four
130 sections from 5 to 10 microns, cut from the original paraffin block. Then, the genomic DNA (gDNA) was
131 eluted in 35 μ L ATE buffer and quantified using the Qubit BR kit (Thermo Fisher Scientific, Waltham,
132 Massachusetts, USA). For cfDNA extraction, 10 to 20 mL peripheral blood was collected in EDTA tubes and
133 processed in less than four hours at the H12O. Samples from Toledo were collected in Roche Cell-Free DNA
134 collection Tubes (Roche Diagnostic, Basel, Switzerland) and sent to the H12O, where plasma separation
135 and cfDNA purification were centralized. There were no differences in cfDNA quantity or quality observed
136 between EDTA and Streck collection tubes. The plasma was separated with two centrifugation steps at
137 1600 g and 4500g, and stored at -80 °C until further use. The purification of cfDNA was performed with a
138 Qiamp Circulating Nucleic Acid kit (Qiagen) and quantified using a Qubit HS kit (Thermo Fisher Scientific).
139 Fragment size and genomic DNA contamination were quantified using a Bioanalyzer 2100 fragment
140 analysis system (Agilent, Santa Clara, California, USA).

141
142 *Baseline Genotyping and LiqBio-MRD Biomarker Selection*

143
144 The lymph node gDNA and plasma cfDNA baseline samples were screened for mutations with a short-
145 length Ampliseq Custom Panel (Thermo-Fisher). The panel, established as a routinary diagnosis tool at the
146 H12O, was designed to cover all coding regions of 56 lymphoma-specific genes in the FFPE samples
147 (Supplemental Table S1). Samples were sequenced with an average coverage of 2,150x on an Ion S5
148 System platform (Life Technologies, Thermo Fisher Scientific). Variant annotation was performed using the
149 default annotate variants single sample workflow from the Ion Reporter software (version 5.18.2.0).
150 Mutations were called when presented more than nine mutated reads and a Variant Allele Frequency

151 (VAF) above $2 \cdot 10^{-2}$ (2%). In the case of FFPE samples, deamination-related base changes were reduced
152 by filtering out C>T / G>A changes with a VAF below $2 \cdot 10^{-1}$ (20%) and a transformed p -value greater than
153 -2 , unless previously described as a somatic aberration in FL (COSMIC database). To select best MRD
154 biomarkers for each patient, we first excluded all potential SNPs, germinal variants and missense variants
155 of unknown significance (VUS) using COSMIC, ClinVar, and dbSNP databases. Then we categorize the
156 remaining somatic mutations based on the number of cancer patients affected and prioritized the ones
157 more frequently involved in lymphoma until we have up to 5-10 markers per patient when possible.
158 (Supplemental Table S2).

159

160 *LiqBio-MRD Methodology and Bioinformatic Pipeline*

161

162 A median of 16.14 ng per mL of plasma (range 2.63-489 ng/mL) was obtained, being the mean amount of
163 cfDNA from the initial 10–20 mL of peripheral blood (PB) of 73.6 ng (range 15.75–1,935 ng). All samples
164 with a gDNA/cfDNA ratio greater than one, calculated using the bioanalyzer electropherogram, were
165 excluded. The minimum quantity of cfDNA targeted for sequencing was 15ng. Considering that a genome
166 equivalent (GE) has a mass of 3pg (31), 15ng is enough to screen 5,000GE and therefore achieve a
167 sensitivity of $2 \cdot 10^{-4}$ VAF (0.02%).

168

169 An amplicon-multiplexed mini-panel was defined for every patient to detect the selected MRD biomarkers
170 identified at diagnosis. The mini-panel included molecular-tagged primer pairs (6-mer tags) to amplify
171 every selected mutation in three biological replicates defined as P1, P2, and P3. (Supplemental Table S3
172 and Figure S2). Then, the three independent tagged post-PCR products were combined in a single tube to
173 continue with sample preparation. Final libraries were sequenced on the Ion S5 System platform (Life
174 Technologies, Thermo Fisher Scientific Inc.) with an estimated depth of 500,000x per amplicon, as
175 previously described (32,33). Despite the dilution curves of 53 genetic variants indicated a potential VAF

176 sensibility below 10^{-4} (Supplemental figure S3), all potential MRD biomarkers were screened with the same
177 pipeline in triplicates of three gDNA samples obtained from healthy control donors. This permitted to
178 define the LOD for every MRD biomarker (mean VAF plus three standard deviations) and exclude all the
179 potential MRD markers that presented a LOD above 10^{-4} (Supplemental Figure S4).

180
181 The FASTQ files produced after sequencing were automatically demultiplexed to separate the reads from
182 the different amplicons and triplicates. To reduce the false positive rate, a strict bioinformatic pipeline was
183 programmed in Python and R to eliminate low-quality reads. The specific wild-type and mutated
184 sequences were generated for each genetic position. These sequences, obtained from the corresponding
185 demultiplexed output file, cover the affected locus with 15 bp upstream and downstream. Only the reads
186 that perfectly match these sequences were considered to calculate the VAF for each triplicate. The noise
187 effects arising from PCR and sequencing were controlled by identifying and removing triplicates that
188 overpassed the mean VAF plus one standard deviation (SD). Finally, the corrected VAF was compared with
189 the LOD calculated for each mutation independently, using three triplicates of three healthy donors as
190 previously explained. The LOD was computed as the mean VAF in control samples plus three times the SD.
191 Every MRD biomarker with a corrected mean VAF below the LOD was automatically eliminated.
192 (Supplemental Table S3) The final LiqBio-MRD value was defined by the mutation with the highest VAF at
193 the sampling time-point, as shown in Supplemental Figure S5.

194
195 *PET/CT Imaging*

196 The PET/CT scans were performed with a General Electric Discovery MI (GEDMI) Scanner or a Siemens
197 Biograph 6 Scanner. PET/CT and CT images were acquired in the same session after injection of 2.5-3
198 MBq/kg ^{18}F -FDG (fluorodeoxyglucose) for the GEDMI Scanner and 4-5 MBq/kg ^{18}F -FDG for the Siemens
199 scanner. All follow-ups were performed in the GEDMI scanner. CT scans obtained with a low-dose protocol

200 were used for attenuation correction of the PET/CT images. Interim and EOT¹⁸FDG-PET/CT scans were
201 visually assessed according to the D5PS, with ¹⁸FDG uptake of any residual lesion, using mediastinal blood
202 pool and liver uptake as reference settings. PET/CT was considered to be positive when the Deauville's
203 score was four or five, and Deauville's scores from one to three were classified as PET/CT negative.

204 In first-line therapy, PET/CT was performed before starting the treatment, after four cycles ($n = 40$), and
205 at the end of treatment (EOT, $n = 54$). After finishing induction, patients were closely monitored with a
206 physical examination and routine laboratory tests. A new scan was performed only when new symptoms
207 or laboratory changes were detected. PET/CT was generally performed at mid-induction ($n = 7$) and EOT
208 ($n = 14$) for patients treated in other lines. The exact time-points are listed in Supplemental Table S4.

209

210 *Statistical Analysis*

211

212 The Kruskal–Wallis test was used to determine statistically significant differences in the obtained samples'
213 MRD values among the PET/CT-related categories. Then, a post hoc Dunn test was conducted to identify
214 the statistically significant pairwise comparisons and the corresponding p -values. The tests were both
215 performed using Python, the prior with the Python package SciPy (version 1.6.2) and the latter with the
216 Python package scikit-posthocs (version 0.6.7). The Pearson correlation coefficient was used to assess the
217 linear relationship between the different variables under study. Univariable Cox proportional hazards
218 regression models and Kaplan–Meier survival analysis were performed to test statistical associations
219 between genetic and imaging findings and survival outcomes. Statistical calculations were conducted using
220 SPSS 22.0 (IBM SPSS Inc, Chicago). P -values of ≤ 0.05 were considered to be significant.

221

222 **Results**

223

224 *Patients' Characteristics and Predictive Features*

225
226 A total of 84 FL patients were included in the study (Supplemental figure S1). The median age was 63 years
227 (35–90 years), and 58% of the patients were female. Eleven cases did not require treatment, 85% of the
228 patients presented low histological grade (1–2), and 79% had advanced (III–IV) Ann Arbor stage (Table 1).
229 Regarding treated cases ($n = 73$), 58 patients received first-line treatment (39 RCHOP, 10 R-bendamustine,
230 4 rituximab monotherapy, and 5 radiotherapy). The other 15 patients were treated with salvage therapy
231 after a previous relapse (Supplemental Table S4). More important prognostic indexes in FL were analyzed.
232 High-risk patients defined by FLIPI, FLIPI2, m7-FLIPI, and PRIMA PI did not show shorter PFS. Bulky disease,
233 the presence of symptoms B, and a lymphocyte-to-monocyte ratio (LMR) of <2.5 were the only variables
234 associated with a higher risk of relapse ($p < 0.05$). After a median follow-up of 22 months (rank 3-61.5), 19
235 patients relapsed after a median of 19 months (16 patients with grade I, II, or 3A and 3 patients
236 transformed). Eight cases died after a median of 29 months (five patients had a low histological grade, and
237 three patients were transformed). The causes of death were lymphoma in four cases (three transformed),
238 infection ($n = 2$), and secondary neoplasia ($n = 1$). Regarding the subgroup of patients treated in first-line
239 therapy ($n=58$) 15 patients relapsed after a median of 12.6 months (3.9-44.9).

240
241 According to the interim evaluation of response in patients treated with first-line therapy ($n=40$), 14
242 patients (35%) reached partial response (PR), and 26 complete response (CR; 65%). At the end of induction
243 treatment ($n=54$), 40 patients reached CR (74%), eight patients PR (15%), one stable disease (SD; 2%) and
244 five progression disease (PD; 9%). In the relapse setting at mid-induction ($n=7$), two patients reached CR
245 (29%), and five PR (71%). At the end of treatment ($n=14$), ten patients achieved CR (72%), one PR (7%) and
246 three PD (21%).

247
248 *Baseline Genotyping on cfDNA Complements Lymph Node Screening in Follicular Lymphoma*

249
250 Baseline genotyping with the targeted NGS panel was performed in 75 lymph node samples and 44 cfDNA
251 plasma samples. In the lymph node samples, 510 mutations were detected with an average of 6.8 somatic
252 mutations per patient (range 0–31) and a mean VAF of 0.31 (range 0.026–1.0). In the cfDNA plasma
253 samples, 144 mutations were detected (average 3.3, range 0–11) with a mean VAF of 0.22 (range 0.025–
254 0.857). Only 4 of 75 (5%) lymph node samples did not present any alteration suitable for MRD monitoring.
255 This number increased to 20% (9 of 44) when only baseline cfDNA was considered. However, somatic
256 mutations were detected in the cfDNA fraction for six of the eight patients without lymph node samples
257 available.

258
259 As previously described (12), the most frequently mutated genes were *KMT2D*, *CREBBP*, *BCL2*, *TNFRSF14*,
260 and *EZH2* (Figure 1A). Although the samples from transformed patients had a similar genetic profile, an
261 increase of *TP53* mutations was observed in this subcohort (3/10, 33% vs. 7/73, 9%, Supplemental Figure
262 S7). Within the 36 cases with available paired lymph node and plasma samples, 88 somatic mutations were
263 identified in both fractions, 33 somatic mutations were only detectable in liquid biopsy, and 160 somatic
264 mutations were only in the lymph node (Supplemental Table S2, Supplemental Figure S6).

265
266 *Clinical Impact of Disease Monitoring by LiqBio-MRD*

267
268 The dynamics of the baseline mutations were analyzed on 151 cfDNA follow-up samples from 54 of 73
269 patients that received treatment (Figure 1B). Additionally, sequential samples of eleven untreated “watch
270 and wait” patients were screened. On average, 3.6 somatic mutations per patient (range 1–12) were
271 selected as MRD biomarkers. Nine mutations were excluded from further analyses as they presented a
272 LOD above $1 \cdot 10^{-4}$. These mutations mainly affected insertions or deletions of one base (Supplemental
273 Figure S4). On the other hand the elimination of outlier triplicates permitted to identify and correct nine

274 false positives follow-up samples. To compare PET/CT and liquid biopsy results, we defined four groups
275 based on the PET/CT data available when the liquid biopsy sample was collected. The first group (complete
276 response, CR) included follow-ups with a Deauville score of 1, 2, or 3 in nodal or extranodal sites with or
277 without a residual mass. The Non-progressive disease group included partial response with a Deauville
278 score 4, or 5 with reduced uptake compared with baseline and residual mass(es). The Progressive disease
279 includes a Deauville score 5 in any lesion with an increase in the intensity of FDG uptake from baseline.
280 The Non-treatment group had samples before treatment started or from untreated patients. (Figure 1C)
281 The LiqBio-MRD values were significantly lower in the CR and Non-progressive disease groups compared
282 to the progressive group ($p < 0.001$ and $p=0.019$, respectively). However, of 53 samples included in the CR
283 group, four were LiqBio-MRD positive. Of note, all samples in "watch and wait" group (eight samples from
284 eight patients) were positive by the LiqBio-MRD test.

285
286 The 54 treated patients with sequential samples available presented an average of three liquid biopsy
287 samples (rank 1–8) after treatment started. Of them, 44 patients were under first-line treatment. To
288 calculate the clinical impact of the LiqBio-MRD test in first-line patients, we defined three different
289 timeframe groups: Early follow-up ($n = 23$) included cfDNA samples from cycles I and II; the interim group
290 ($n = 23$) included samples obtained in cycles III and IV; the final or EOT group included 32 cfDNA samples
291 obtained in cycle VI or the first sample available under maintenance (Figure 2, left). Positive LiqBio-MRD
292 values in the early group did not increase the risk of progression ($HR_{EARLY} 2.3$, 95% CI 0.44–11.8, $p = 0.310$).
293 This tendency changed at interim monitoring ($HR_{INT} 11.0$, 95% CI 2.10–57.7, $p = 0.005$). The differences
294 between LiqBio-MRD positive and negative cases were even more pronounced at EOT (HR_{EOT} , HR 19.1,
295 95% CI 4.10–89.4, $p < 0.001$), Figure 2, right). The results of the entire cohort, including relapsed patients,
296 are shown in Supplemental Figure S8.

297

298 *Interim Monitoring by PET/CT of Previously Untreated Patients Predicts Progression*

299
300 PET/CT D5PS tests also showed prognostic value at interim evaluation. PET/CT positive cases had a mPFS_{INT}
301 of 19 months vs. NR ($p < 0.001$, Figure 3A). Comparable results were observed at EOT (mPFS_{EOT} PET/CT 13
302 months vs. NR, $p < 0.001$, Figure 3B), and when relapsed patients were included (Supplemental Figure S8).
303 Of note, the distribution of cases according to interim and EOT TPs for PET/CT and LiqBio-MRD presented
304 a concordance of 76% (Kappa = 0.401).

305

306 *The Combination of LiqBio-MRD and PET/CT Identifies POD24 Patients*

307

308 Next, we studied the 41 first-line patients with data available on both PET/CT and LiqBio-MRD. The last TP
309 (interim or EOT) with data for both tests was considered for this analysis. Twenty-six patients were
310 negative by both techniques, seven were positive, and eight presented discordant results. Considering
311 only concordant results ($n=33$), the combination of both tests showed a sensitivity (SE) of 88% and a
312 specificity (SP) of 100%, with a PPV of 100% and NPV of 96%. Strikingly, all positive patients by both tests
313 had a 2-year PFS below 24 months (mPFS of 7 months for +/+ vs. NA for -/- cases, $p < 0.001$, Figure 4).
314 Moreover, the only case (FL25) that progressed with a negative result by both tests, was positive in a
315 sequential cfDNA sample obtained at maintenance, five months before progression. Regarding the eight
316 cases with discordant results (20%), six patients were incorrectly classified by PET/CT, and only two
317 patients were incorrectly classified by LiqBio-MRD (Figure 4). The results including relapsed patients are
318 shown in Supplemental Figure S9.

319

320 Other approaches for disease monitoring were also tested. Flow cytometry data was only available for
321 eleven patients with bone marrow infiltration. Two patients were positive at follow-up and nine patients
322 were negative at follow-up, concurring at 100% with PET/CT and LiqBio-MRD. The BCL2/IgH
323 rearrangements were screened in 33 patients with peripheral blood samples available. Rearrangements

324 were only detected at baseline diagnosis for ten of the patients, being all negative in follow-up samples.
325 Two of these cases were positive by PET/CT and LiqBioMRD, four cases presented discordant results, and
326 three cases were negative by both tests.

327

328 *Dynamics of Somatic Mutations during the Follow-up of FL Patients*

329

330 As indicated above, only one patient (FL25) had a negative result by PET/CT and LiqBio-MRD at interim and
331 EOT and eventually progressed. Three somatic mutations affecting *KMT2D*, *CREBBP*, and *ARID1A* were
332 found in this case. Of interest, this patient was MRD negative in three TPs obtained during the first year
333 but had a positive LiqBio-MRD sample obtained 15 months after the start of treatment. An additional
334 positive liquid biopsy was received three months later, and PET/CT was performed, confirming progression
335 but with a low tumor burden (Figure 5A). The patient continued maintenance therapy, achieving a
336 complete response a few months later.

337

338 The opposite dynamics were observed in patient FL5. This patient did not respond to RCHOP (DS5) and
339 received R-bendamustine as second-line therapy. The interim PET/CT showed a poor response (DS5), and
340 the biopsy confirmed the transformation to high-grade lymphoma. After failure of rescue treatment with
341 R-GEMOX-dexamethasone and R-polatuzumab bendamustine, the patient received radiotherapy where a
342 reduction in the main clone was observed (Figure 5B). Of note, the clone detected in cfDNA disappeared
343 under first-line therapy.

344

345 Patient FL30 presented two mutations detected only in lymph node and two more only detected in cfDNA.
346 In follow-up samples, the four mutations were undetectable. In the PET/CT evaluation, a residue was
347 observed in the scans, complicating the interpretation of the imaging results (Figure 5C). This patient is
348 still in CR after two years of follow-up.

349
350 Although a solid biopsy was unavailable for patient FL31, six somatic mutations were detected in the
351 baseline liquid biopsy sample. In follow-up cfDNA samples, despite an initial reduction during the first two
352 cycles, a rapid increase in the disease burden after cycle III was observed. The patient progressed in cycle
353 VI and died under rescue therapy only nine months from the start of the treatment (Figure 5D). The
354 dynamics of all the treated patients with follow-up samples available are shown in Supplemental Figure
355 S9.

356

357 **Discussion**

358

359 This prospective study evaluates, for the first time, the usefulness of liquid biopsy MRD by ultra-deep
360 sequencing in combination with D5PS PET/CT to identify, early on, those FL patients with a high risk of
361 relapse in less than 24 months (POD24). Our approach is based on the use of somatic mutations as disease
362 biomarkers, as we previously described for acute myeloid leukemia (32). First, we screened baseline lymph
363 node and plasma samples to identify patient specific biomarkers. The genetic profile of our cohort mimics
364 the one previously described by Pastore et al. (12) but with an expected increase of *TP53* alterations in
365 transformed cases (34) (Supplemental Figure S1). Although the custom DNA panel was initially designed
366 for FFPE samples, the small amplicon size permitted the detection of lymphoma-specific mutations in
367 baseline liquid biopsies (Figure 1A). In our study, limited by the follow-up and the small and heterogeneous
368 number of subjects, the only clinically relevant prognostic factor for PFS in newly diagnosed patients ($n =$
369 84) was the low lymphocyte-to-monocyte ratio (19). We did not find prognostic differences by applying
370 IPI, FLIPI, FLIPI2, m7-FLIPI, or PRIMA IPI. However, somatic mutations suitable for LiqBio-MRD monitoring
371 were found in 95% of patients with lymph node samples and 80% of patients with liquid biopsy samples
372 available. Our results indicate that follicular lymphoma gene driver mutations are detectable in liquid
373 biopsy. Still, more sensitive approaches are needed. In any case, the number of patients with potential

374 MRD biomarkers considerably improves the applicability of MRD assessment compared to other described
375 techniques, such as PCR of the IGH/BCL2 translocation (20,29). Although PCR-positive is predictive of lower
376 PFS, a considerable number of patients are t(14;18) negative (60%). Moreover, FL is a predominantly nodal
377 disease, and the absence of t(14;18) in bone marrow does not adequately reflect the response status (41).
378 Further, t(14;18) can also be found in healthy individuals at low level.

379
380 In this study, LiqBio-MRD was evaluated in the plasma of 54 patients that received treatment (43 first-line
381 therapy). The analysis, performed in 151 follow-up cfDNA samples allowed us to define patient-specific
382 disease dynamics (Figure 1B, Supplemental Figure S7) and their correlation with the clinical outcome
383 (Figure 1C). To the best of our knowledge, there are no studies in FL evaluating early MRD assessed by
384 liquid biopsy. Conversely, there are already some studies in DLBCL (24,35,36) and Hodgkin lymphoma (37)
385 where it is known that levels often change rapidly after the initiation of therapy. Following this hypothesis
386 in FL, we performed an early LiqBio-MRD evaluation (Cycle 2) on 23 patients. Although a trend to shorter
387 PFS was observed in MRD-positive cases, 6 of 13 cases eventually became negative at later time points
388 (Figure 2), suggesting that FL presents a different dynamic than DLBCL (38) and treatment need longer to
389 cleanse the tumor.

390
391 Since the Lugano classification, the criteria to determine the quality of treatment response rely on the
392 D5PS PET/CT evaluation (38). Several studies, including large retrospective subanalyses of randomized
393 trials have shown that PET/CT negativity correlates solidly with PFS (25,39). Nevertheless, the use of
394 PET/CT alone is hampered by its limited sensitivity and specificity and the interpretation of the results
395 being highly dependent on the evaluating radiologist (27,40). Consistent with previous reports (23), from
396 the 64 patients with available PET/CT scans at WOT (50 patients in first-line therapy), 70% of the patients
397 reached a CR.

398

399 On the other hand, the LiqBio-MRD test showed an extraordinary capacity to identify patients at risk of
400 progression after only four cycles of RCHOP (Figure 3A). Comparable results were observed by interim
401 PET/CT (Figure 3B). This result suggests that LiqBio-MRD or PET/CT interim evaluation should be
402 considered in future clinical trial settings. Regarding EOT evaluation, both tests segregated high-risk
403 patients (Figure 3C, D). Although similar results have already been shown in FL patients using PCR-based
404 MRD techniques, these approaches were hampered by a lower applicability (20,29,41–43).

405
406 PET/CT has only been used in combination with PCR in a small exploratory analysis and MRD refined the
407 predictive power of PET/CT (29). However, no combination of PET/CT and MRD strategies has been
408 reported using NGS liquid biopsy techniques. In our study, the combination of both methods identified
409 100% of the POD24 patients. As shown in Figure 4, patients with concordant results ($n = 28$) were almost
410 perfectly segregated. These results remained after excluding transformed cases (Supplemental Figure S8).
411 The only double negative patient (FL25, Figure 5A) that progressed presented an increase in tumor burden
412 detectable by LiqBio-MRD five months before progression in a sample obtained within maintenance. This
413 suggests that sequential monitoring with a minimally invasive test such as LiqBio-MRD may be essential to
414 identify POD24 cases and anticipate patients' relapses. Another interesting case, FL5, illustrates how
415 LiqBio-MRD may have other possible applications (Figure 5B). In this chemo-refractory patient,
416 radiotherapy had an abscopal effect, confirmed by the rapid descend of ctDNA not otherwise explicated
417 (44).

418
419 Our study has several limitations, including the limited number of patients, the heterogenous treatment
420 administered, and the absence of available tests in all the time-points. However, several factors permitted
421 the development of a LiqBio-MRD test with extraordinary performance. First, the MRD amplicons were
422 designed shorter than 120bp and all MRD samples screened presented at least 15ng of cfDNA to guaranty
423 the amplification of enough tumor cfDNA molecules. More importantly, the use of triplicates and the

424 definition of LOD in healthy control donors permitted to identify and correct the false positive values
425 induced by PCR and sequencing errors or the variant intrinsic noise due to the genetic context. Although
426 it seems mandatory to perform larger studies to confirm this preliminary data, our results demonstrate,
427 for the first time, that NGS-based MRD quantification is feasible in liquid biopsies from FL. The
428 achievement of negative ctDNA after treatment and in an interim analysis enhances prognostic
429 information on the patients' outcomes, both in first-line therapy and at relapse. PET/CT and LiqBio-MRD
430 can synergistically contribute to predicting progression and POD24 with high sensitivity and specificity.
431 Additionally, this test better reflects intra-patient tumor heterogeneity (45,46) and could be used to detect
432 drug resistance, high-risk transformation and guide and monitor treatment.

433
434 In conclusion, LiqBio-MRD monitoring in FL represents a promising option, complementary to metabolic
435 imaging, to identify patients at high risk of failure early on during treatment and is a useful approach to
436 response-adapted precision therapy to be considered in clinical trials.

437

438 **Acknowledgements**

439 This study has been funded by Instituto de Salud Carlos III (ISCIII) and co-funded by the European Union
440 through the projects PI21/00314, PI 19/01430, PI19/01518 and PI18/00295, PTQ2020-011372,
441 CP19/00140, CP22/00082, Doctorado industrial CAM IND2020/TIC-17402 and CRIS cancer foundation.

442

443 **Author Contributions**

444 AJU, MP, IR, MG, RA, JML and SB designed the research. JC, RS, LR, AJ and MR performed the experiments.
445 AM, YR, SD and JMR, CW, PT and SB defined the bioinformatic pipeline and performed sequencing data
446 analysis. AJU, MP, GF, AR, CB, LPN, CG, MM, LFC, MC, TB, MG, PS and RS provided patient samples and
447 clinical data. All authors analyzed and interpreted the data. AJU, MP, AM and SB wrote the manuscript
448 which was approved by all authors.

449

450 **Competing Interests**

451 RA, JML and SB are equity shareholders of Altum Sequencing Co. LFC received honoraria and received
452 research funding from Roche, Novartis, Astra Zeneca, Janssen, BMS, Pfizer and Incyte. The remaining
453 authors declare no competing financial interests.

454

455 **Data Availability Statement**

456 The datasets generated during and/or analyzed during the current study are available from the
457 corresponding author on reasonable request.

458

459 **References**

460

- 461 1. Anderson JR, Armitage JO, Weisenburger DD. Epidemiology of the non-Hodgkin's lymphomas:
462 Distributions of the major subtypes differ by geographic locations. *Ann Oncol.* 1998 Jul;9(7).
- 463 2. Küppers R, Stevenson FK. Critical influences on the pathogenesis of follicular lymphoma. *Blood.*
464 2018 May 24;131(21):2297–306.
- 465 3. Cheah CY, Chihara D, Ahmed M, Davis RE, Nastoupil LJ, Phansalkar K, et al. Factors influencing
466 outcome in advanced stage, low-grade follicular lymphoma treated at MD Anderson Cancer
467 Center in the rituximab era. *Ann Oncol.* 2016 May;27(5).
- 468 4. Jiménez-Ubieto A, Grande C, Caballero D, Yáñez L, Novelli S, Hernández-Garcia MT, et al.
469 Autologous Stem Cell Transplantation for Follicular Lymphoma: Favorable Long-Term Survival
470 Irrespective of Pretransplantation Rituximab Exposure. *Biol Blood Marrow Transplant.* 2017
471 Oct;23(10).
- 472 5. Jiménez-Ubieto A, Grande C, Caballero D, Yáñez L, Novelli S, Hernández MT, et al. Progression-
473 free survival at 2 years post-autologous transplant: a surrogate end point for overall survival in

- 474 follicular lymphoma. *Cancer Med.* 2017 Dec 1;6(12):2766–74.
- 475 6. Casulo C, Dixon JG, Le-Rademacher J, Hoster E, Hochster H, Hiddemann W, et al. Validation of
476 POD24 As a Robust Early Clinical Endpoint of Poor Survival in FL from 5,225 Patients on 13 Clinical
477 Trials. *Blood.* 2021 Oct 6;
- 478 7. Pasqualucci L, Khiabani H, Fangazio M, Vasishtha M, Messina M, Holmes AB, et al. Genetics of
479 Follicular Lymphoma Transformation. *Cell Rep.* 2014;6(1):130–40.
- 480 8. Sarkozy C, Trneny M, Xerri L, Wickham N, Feugier P, Leppa S, et al. Risk factors and outcomes for
481 patients with follicular lymphoma who had histologic transformation after response to first-line
482 immunochemotherapy in the PRIMA trial. *J Clin Oncol.* 2016 Aug 1;34(22):2575–82.
- 483 9. Sorigue M, Mercadal S, Alonso S, Fernández-Álvarez R, García O, Moreno M, et al. Refractoriness
484 to immunochemotherapy in follicular lymphoma: Predictive factors and outcome. *Hematol Oncol.*
485 2017 Dec 1;35(4):520–7.
- 486 10. Alonso-Álvarez S, Magnano L, Alcoceba M, Andrade-Campos M, Espinosa-Lara N, Rodríguez G, et
487 al. Risk of, and survival following, histological transformation in follicular lymphoma in the
488 rituximab era. A retrospective multicentre study by the Spanish GELTAMO group. *Br J Haematol.*
489 2017 Sep 1;178(5):699–708.
- 490 11. Okosun J, Bödör C, Wang J, Araf S, Yang CY, Pan C, et al. Integrated genomic analysis identifies
491 recurrent mutations and evolution patterns driving the initiation and progression of follicular
492 lymphoma. *Nat Genet.* 2014 Feb;46(2):176–81.
- 493 12. Pastore A, Jurinovic V, Kridel R, Hoster E, Staiger AM, Szczepanowski M, et al. Integration of gene
494 mutations in risk prognostication for patients receiving first-line immunochemotherapy for
495 follicular lymphoma: A retrospective analysis of a prospective clinical trial and validation in a
496 population-based registry. *Lancet Oncol.* 2015 Sep 1;16(9):1111–22.
- 497 13. Jurinovic V, Kridel R, Staiger AM, Szczepanowski M, Horn H, Dreyling MH, et al. Clinicogenetic risk
498 models predict early progression of follicular lymphoma after first-line immunochemotherapy.

- 499 Blood. 2016 Aug 25;128(8):1112–20.
- 500 14. Meignan M, Cottereau AS, Versari A, Chartier L, Dupuis J, Boussetta S, et al. Baseline metabolic
501 tumor volume predicts outcome in high-tumor-burden follicular lymphoma: A pooled analysis of
502 three multicenter studies. In: Journal of Clinical Oncology. American Society of Clinical Oncology;
503 2016. p. 3618–26.
- 504 15. Cottereau AS, Versari A, Chartier L, Dupuis J, Tarantino V, Casasnovas R-O, et al. Low Suvmax
505 Measured on Baseline FDG-PET/CT and Elevated $\beta 2$ Microglobulin Are Negative Predictors of
506 Outcome in High Tumor Burden Follicular Lymphoma Treated By Immunochemotherapy: A
507 Pooled Analysis of Three Prospective Studies. Blood. 2016 Dec 2;128(22):1101–1101.
- 508 16. Bachy E, Maurer MJ, Habermann TM, Gelas-Dore B, Maucort-Boulch D, Estell JA, et al. A simplified
509 scoring system in de novo follicular lymphoma treated initially with immunochemotherapy.
510 Blood. 2018 Jul 5;132(1):49–58.
- 511 17. Huet S, Tesson B, Jais JP, Feldman AL, Magnano L, Thomas E, et al. A gene-expression profiling
512 score for prediction of outcome in patients with follicular lymphoma: a retrospective training and
513 validation analysis in three international cohorts. Lancet Oncol. 2018 Apr 1;19(4):549–61.
- 514 18. Mir F, Barrington SF, Brown H, Nielsen T, Sahin D, Meignan M, et al. Baseline SUVmax did not
515 predict histological transformation in follicular lymphoma in the phase 3 GALLIUM study. Blood.
516 2020 Apr 9;135(15):1214–8.
- 517 19. Mozas P, Rivero A, Rivas-Delgado A, Nadeu F, Clot G, Correa JG, et al. A low lymphocyte-to-
518 monocyte ratio is an independent predictor of poorer survival and higher risk of histological
519 transformation in follicular lymphoma. Leuk Lymphoma. 2021;62(1):104–11.
- 520 20. Luminari S, Manni M, Galimberti S, Versari A, Tucci A, Boccomini C, et al. Response-Adapted
521 Postinduction Strategy in Patients With Advanced-Stage Follicular Lymphoma: The FOLL12 Study.
522 J Clin Oncol. 2022 Mar 1;40(7):729–39.
- 523 21. Delfau-Larue MH, Van Der Gucht A, Dupuis J, Jais JP, Nel I, Beldi-Ferchiou A, et al. Total metabolic

- 524 tumor volume, circulating tumor cells, cell-free DNA: Distinct prognostic value in follicular
525 lymphoma. *Blood Adv.* 2018 Apr 10;2(7):807–16.
- 526 22. Sarkozy C, Huet S, Carlton VEH, Fabiani B, Delmer A, Jardin F, et al. The prognostic value of clonal
527 heterogeneity and quantitative assessment of plasma circulating clonal IG-VDJ sequences at
528 diagnosis in patients with follicular lymphoma. *Oncotarget.* 2017 Jan 31;8(5):8765–74.
- 529 23. Kurtz DM, Green MR, Bratman S V., Scherer F, Liu CL, Kunder CA, et al. Noninvasive monitoring of
530 diffuse large B-cell lymphoma by immunoglobulin high-throughput sequencing. *Blood.* 2015 Jun
531 11;125(24):3679–87.
- 532 24. Kurtz DM, Soo J, Co Ting Keh L, Alig S, Chabon JJ, Sworder BJ, et al. Enhanced detection of minimal
533 residual disease by targeted sequencing of phased variants in circulating tumor DNA. *Nat*
534 *Biotechnol* 2021 3912. 2021 Jul 22;39(12):1537–47.
- 535 25. Trotman J, Barrington SF, Belada D, Meignan M, MacEwan R, Owen C, et al. Prognostic value of
536 end-of-induction PET response after first-line immunochemotherapy for follicular lymphoma
537 (GALLIUM): secondary analysis of a randomised, phase 3 trial. *Lancet Oncol.* 2018 Nov
538 1;19(11):1530–42.
- 539 26. Dupuis J, Berriolo-Riedinger A, Julian A, Brice P, Tychyj-Pinel C, Tilly H, et al. Impact of
540 [18F]fluorodeoxyglucose positron emission tomography response evaluation in patients with
541 high-tumor burden follicular lymphoma treated with immunochemotherapy: A prospective study
542 from the Groupe d'Etudes des Lymphomes de l'Adulte and GOELAMS. *J Clin Oncol.* 2012 Dec
543 10;30(35):4317–22.
- 544 27. Han HS, Escalón MP, Hsiao B, Serafini A, Lossos IS. High incidence of false-positive PET scans in
545 patients with aggressive non-Hodgkin's lymphoma treated with rituximab-containing regimens.
546 *Ann Oncol.* 2009 Feb 1;20(2):309–18.
- 547 28. Ansell SM, Armitage JO. Positron emission tomographic scans in lymphoma: Convention and
548 controversy. In: *Mayo Clinic Proceedings.* Elsevier Ltd; 2012. p. 571–80.

- 549 29. Luminari S, Galimberti S, Versari A, Biasoli I, Anastasia A, Rusconi C, et al. Positron emission
550 tomography response and minimal residual disease impact on progression-free survival in
551 patients with follicular lymphoma. A subset analysis from the FOLL05 trial of the fondazione
552 italiana linfomi. Vol. 101, Haematologica. Ferrata Storti Foundation; 2016. p. e66–8.
- 553 30. Brice P, Bastion Y, Lepage E, Brousse N, Haioun C, Moreau P, et al. Comparison in low-tumor-
554 burden follicular lymphomas between an initial no-treatment policy, prednimustine, or interferon
555 alfa: a randomized study from the Groupe d'Etude des Lymphomes Folliculaires. Groupe d'Etude
556 des Lymphomes de l'Adulte. J Clin Oncol. 1997;15(3):1110–7.
- 557 31. Dang DK, Park BH. Circulating tumor DNA: current challenges for clinical utility. J Clin Invest. 2022
558 Jun 15;132(12).
- 559 32. Onecha E, Linares M, Rapado I, Ruiz-Heredia Y, Martinez-Sanchez P, Cedena T, et al. A novel deep
560 targeted sequencing method for minimal residual disease monitoring in acute myeloid leukemia.
561 Haematologica. 2019 Jan 31;104(2):288.
- 562 33. Sánchez R, Dorado S, Ruíz-Heredia Y, Martín-Muñoz A, Rosa-Rosa JM, Ribera J, et al. Detection of
563 kinase domain mutations in BCR::ABL1 leukemia by ultra-deep sequencing of genomic DNA. Sci
564 Rep. 2022 Dec 1;12(1).
- 565 34. Bouska A, McKeithan TW, Deffenbacher KE, Lachel C, Wright GW, Iqbal J, et al. Genome-wide
566 copy-number analyses reveal genomic abnormalities involved in transformation of follicular
567 lymphoma. Blood. 2014 Mar 13;123(11):1681–90.
- 568 35. Kurtz DM, Scherer F, Jin MC, Soo J, Craig AFM, Esfahani MS, et al. Circulating tumor DNA
569 measurements as early outcome predictors in diffuse large B-cell lymphoma. J Clin Oncol. 2018
570 Oct 1;36(28):2845–53.
- 571 36. Roschewski M, Dunleavy K, Pittaluga S, Moorhead M, Pepin F, Kong K, et al. Circulating tumour
572 DNA and CT monitoring in patients with untreated diffuse large B-cell lymphoma: A correlative
573 biomarker study. Lancet Oncol. 2015;16(5):541–9.

- 574 37. Spina V, Brusca A, Cuccaro A, Martini M, Trani M Di, Forestieri G, et al. Circulating tumor DNA
575 reveals genetics, clonal evolution, and residual disease in classical Hodgkin lymphoma. *Blood*.
576 2018 May 31;131(22):2413–25.
- 577 38. Cheson BD, Fisher RI, Barrington SF, Cavalli F, Schwartz LH, Zucca E, et al. Recommendations for
578 initial evaluation, staging, and response assessment of Hodgkin and non-Hodgkin lymphoma: the
579 Lugano classification. *J Clin Oncol*. 2014 Sep 20;32(27):3059–67.
- 580 39. Dupuis J, Berriolo-Riedinger A, Julian A, Brice P, Tychyj-Pinel C, Tilly H, et al. Impact of
581 [(18)F]fluorodeoxyglucose positron emission tomography response evaluation in patients with
582 high-tumor burden follicular lymphoma treated with immunochemotherapy: a prospective study
583 from the Groupe d'Etudes des Lymphomes de l'Adulte and GOELAMS. *J Clin Oncol*. 2012 Dec
584 10;30(35):4317–22.
- 585 40. Ansell SM, Armitage JO. Positron emission tomographic scans in lymphoma: convention and
586 controversy. *Mayo Clin Proc*. 2012;87(6):571–80.
- 587 41. Galimberti S, Luminari S, Ciabatti E, Grassi S, Guerrini F, Dondi A, et al. Minimal residual disease
588 after conventional treatment significantly impacts on progression-free survival of patients with
589 follicular lymphoma: The FIL FOLL05 trial. *Clin Cancer Res*. 2014 Dec 15;20(24):6398–405.
- 590 42. Zohren F, Bruns I, Pechtel S, Schroeder T, Fenk R, Czibere A, et al. Prognostic value of circulating
591 Bcl-2/IgH levels in patients with follicular lymphoma receiving first-line immunochemotherapy.
592 *Blood*. 2015 Sep 17;126(12):1407–14.
- 593 43. Pott C, Hoster E, Kehden B, Unterhalt M, Herold M, van der Jagt RH, et al. Minimal Residual
594 Disease in Patients with Follicular Lymphoma Treated with Obinutuzumab or Rituximab As First-
595 Line Induction Immunochemotherapy and Maintenance in the Phase 3 GALLIUM Study. *Blood*.
596 2016 Dec 2;128(22):613–613.
- 597 44. Siva S, MacManus MP, Martin RF, Martin OA. Abscopal effects of radiation therapy: a clinical
598 review for the radiobiologist. *Cancer Lett*. 2015 Jan 1;356(1):82–90.

- 599 45. Roschewski M, Rossi D, Kurtz DM, Alizadeh AA, Wilson WH. Circulating Tumor DNA in Lymphoma:
600 Principles and Future Directions. *Blood cancer Discov.* 2022 Jan;3(1):5–15.
- 601 46. Scherer F, Kurtz DM, Newman AM, Stehr H, Craig AFM, Esfahani MS, et al. Distinct biological
602 subtypes and patterns of genome evolution in lymphoma revealed by circulating tumor DNA. *Sci*
603 *Transl Med.* 2016 Nov 9;8(364).

604

605

606 **Figure 1.** Baseline genotyping and potential of the liquid biopsy MRD test (LiqBio-MRD) to monitor disease
607 progression: **(A)** Oncoplot of the baseline genotyping of 75 lymph node solid biopsy samples (red) and 44
608 plasma liquid biopsy samples (yellow). Patients are represented in the X-axis, genes in the Y-axis; **(B)**
609 Dynamics of circulating free DNA (cfDNA) quantified by LiqBio-MRD in 55 Follicular Lymphoma (FL)
610 patients. The LiqBio-MRD values for each follow-up datapoint (Y-axis) are plotted against the month from
611 treatment start (X-axis), patients that progressed are represented in red, complete and partial responses
612 are represented in blue. **(C)** Correlation of Liqbio-MRD and PET/CT. The complete response (CR) included
613 follow-ups with a Deauville score of 1, 2, or 3 in nodal or extranodal sites with or without a residual mass.
614 The Non-progressive disease (excluding CR) group included partial response cases with Deauville score of
615 4, or 5 with reduced uptake compared with baseline and residual mass(es). The progressive disease
616 includes a Deauville score 4 or 5* in any lesion with an increase in the intensity of FDG uptake from
617 baseline.

618

619 **Figure 2.** Clinical impact of early monitoring by LiqBio-MRD: **(left)** Swimmer plot of the different follow-up
620 time-points screened for all patients under first-line treatment included in the survival analysis. Red boxes
621 represent time-points with positive Minimal Residual Disease (MRD) value. Blue boxes, samples with
622 negative MRD value. The samples used in the survival analysis at Early (E, 1-2 RCHOP cycles), Interim (I, 3-
623 4 RCHOP cycles) and Final (F) or end of treatment (EOT, 5-6 RCHOP cycles) time-points are indicated for

624 each patient. **(Right)** Kaplan–Mayer curves of the impact of LiqBio-MRD monitoring at the different time-
625 points. These analyses were performed with all the patients under first-line treatment.

626
627 **Figure 3.** Interim monitoring by PET/CT predicts progression in first-line treated patients. Kaplan–Meier
628 curves showing the impact of interim**(A)** and end of treatment (EOT) **(B)** monitoring by PET/CT scan in
629 patients under first-line therapy.

630
631 **Figure 4.** Clinical Impact of the LiqBio-MRD and PET/CT combination in first-line therapy. Kaplan–Meier
632 curves show the capacity to identify patients that progress during the first two years after first-line therapy
633 (POD24) when both tests are combined. An analysis was performed using the last time-point with both
634 determinations available (interim or EOT).

635
636 **Figure 5.** Examples of the disease dynamics monitored by LiqBio-MRD. The left panel represents the
637 baseline genotyping of lymph nodes (SolBio) and plasma cfDNA (LiqBio) samples after applying the low
638 sensitive targeted panel (sensitivity $2 \cdot 10^{-2}$). The panel in the middle represents the variant allele frequency
639 (VAF) values of the different mutations obtained by the ultrasensitive LiqBio-MRD test (sensitivity $2 \cdot 10^{-4}$).
640 The right panel represents the limit of detection (LOD; mean + three standard deviations) defined in
641 healthy control datapoints for every tracked mutation. Mutations with LOD above $1 \cdot 10^{-4}$, represented with
642 dotted lines, were not used for MRD value calculation. RCHOP: cyclophosphamide/doxorubicin/
643 prednisone/rituximab/vincristine. R-Benda: rituximab/bendamustine. Pola: polatuzumab. GEMOX:
644 gemcitabine/oxaplatin. Dexa: Dexamethasone.

645
646 **Table 1.** Patient characteristics.

		All series (n=84) *	First-line therapy (n=58)	Other lines of therapy (n=15) **
Age (y), median (rank)		63 (35-90)	65 (37-86)	62 (44-90)
Male gender		35/84 (42%)	27/58 (47%)	4/15 (27%)
Median follow-up since treatment (months)		-	20.5 (3-61.5)	31 (5-45.3)
Ann-Arbor Stage ≥3		66/84 (79%)	46/58 (79%)	14/15 (93%)
Histological grade	1-2	71/84 (85%)	51/58 (88%)	11/15 (73%)
	3A	4/84 (5%)	2/58 (3%)	1/15 (7%)
	3B	1/84 (1%)	1/58 (2%)	1/15 (7%)
	Transformed	7/84 (9%)	4/58 (7%)	3/15 (20%)
B symptoms		27/84 (32%)	16/58 (28%)	10/15 (66%)
ECOG-PS ≥ 2		9/84 (11%)	5/58 (9%)	4/15 (27%)
Bulky disease		17/84 (20%)	14/58 (24%)	3/15 (20%)
Bone marrow involvement		34/83 (41%)	23/58 (40%)	8/15 (53%)
Haemoglobin < 12 g/dL		12/84 (14%)	8/58 (14%)	4/15 (27%)
Lactate dehydrogenase >UNL		33/84 (39%)	26/58 (45%)	3/15 (20%)
B₂-microglobulin elevated		31/77 (40%)	24/55 (44%)	3/11 (28%)
FLIPI risk	Low	16/84 (19%)	9/53 (17%)	5/15 (33%)
	Intermediate	30/84 (36%)	17/53 (32%)	4/15 (27%)
	High	38/84 (45%)	27/53 (51%)	6/15 (40%)
FLIPI2 risk	Low	39/71 (55%)	25/55 (43%)	5/10 (50%)
	Intermediate	17/71 (24%)	13/55 (24%)	4/10 (40%)
	High	15/71 (21%)	12/55 (23%)	1/10 (10%)
PRIMA PI	Low	39/77 (51%)	25/55 (51%)	4/10 (40%)
	Intermediate	17/77 (22%)	10/55 (18%)	3/10 (30%)
	High	21/77 (27%)	17/55 (31%)	3/10 (30%)
Lymphocyte to monocyte ratio < 2.5		29/84 (34.5%)	21/58 (36%)	5/15 (33%)

* Eleven patients in “watch and wait” policy at the time of analysis

** Eight patients with two previous therapy lines and six with three or more (see supplementary table 4)

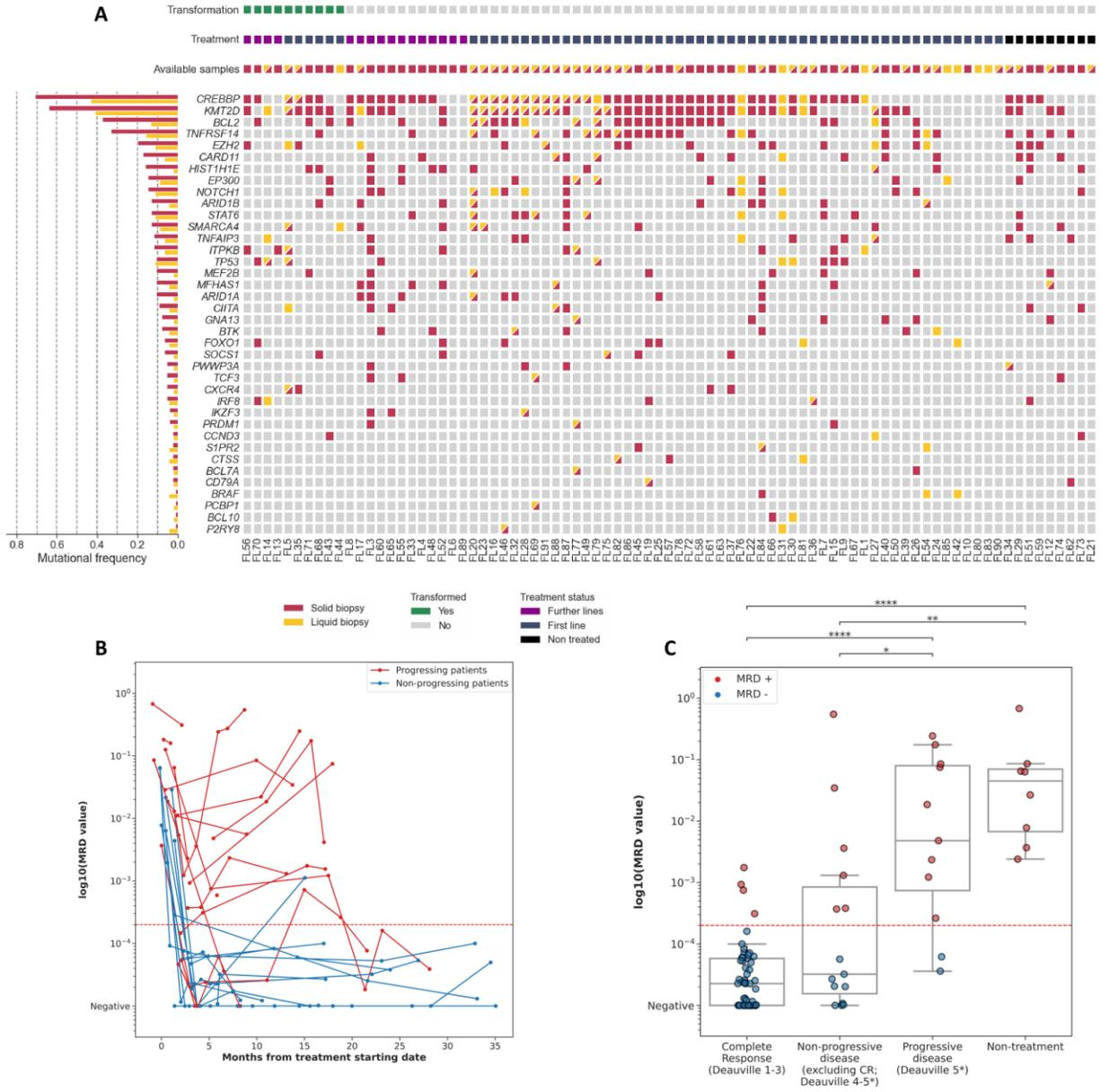
647

648

649 **Figures**

650

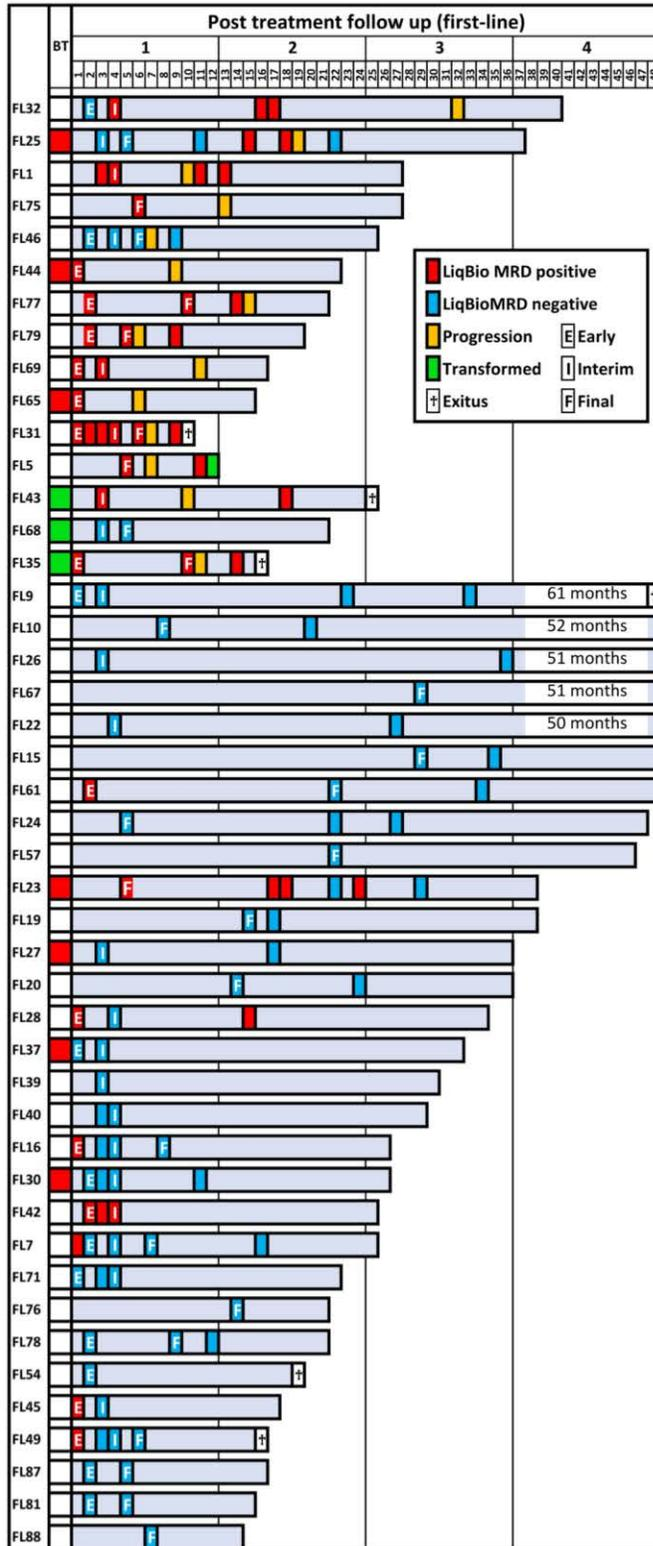
Figure 1



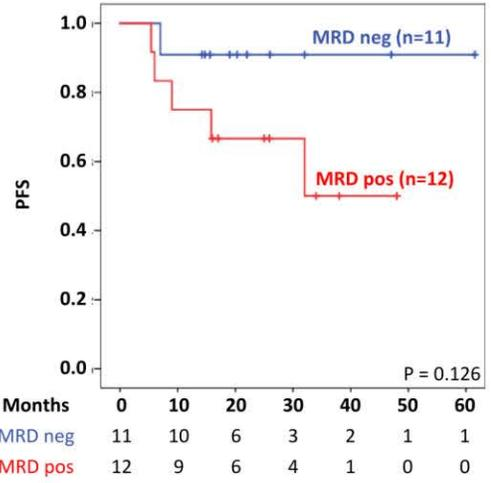
651

652

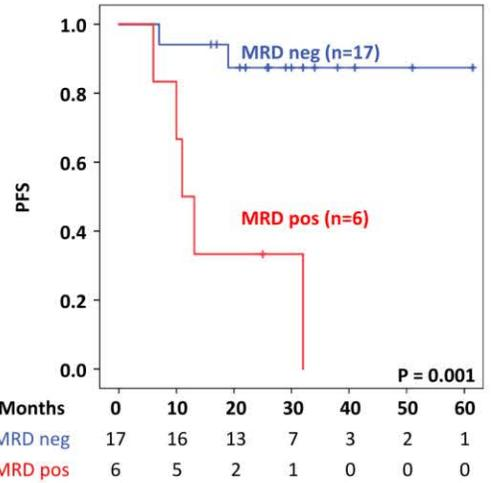
Figure 2



Early LiqBio-MRD.



Interim LiqBio-MRD.



Final LiqBio-MRD (EOT).

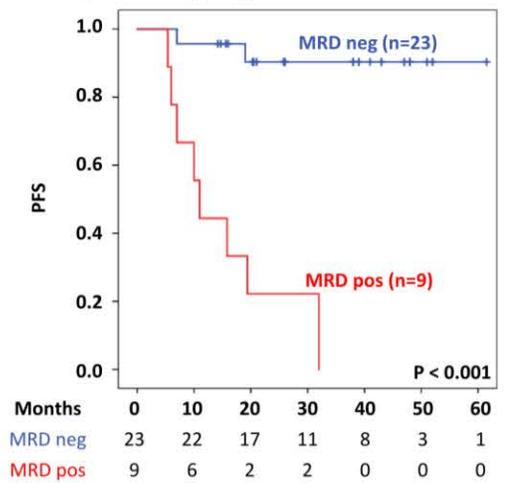
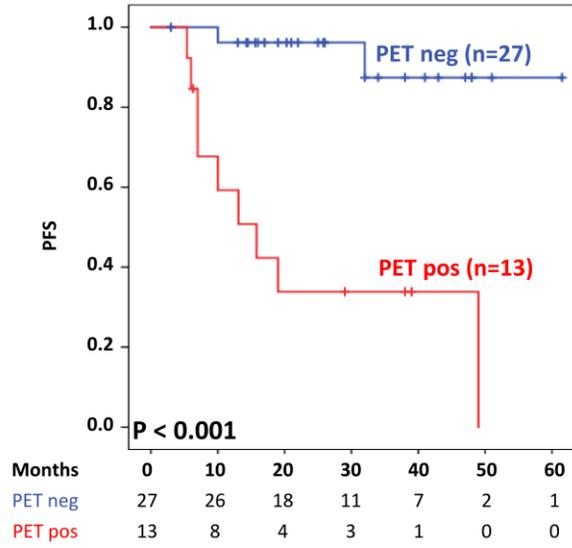
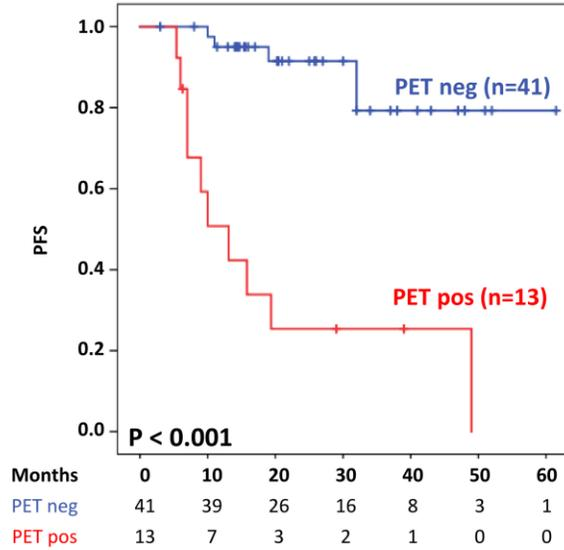


Figure 3

A. PET/CT interim. First line



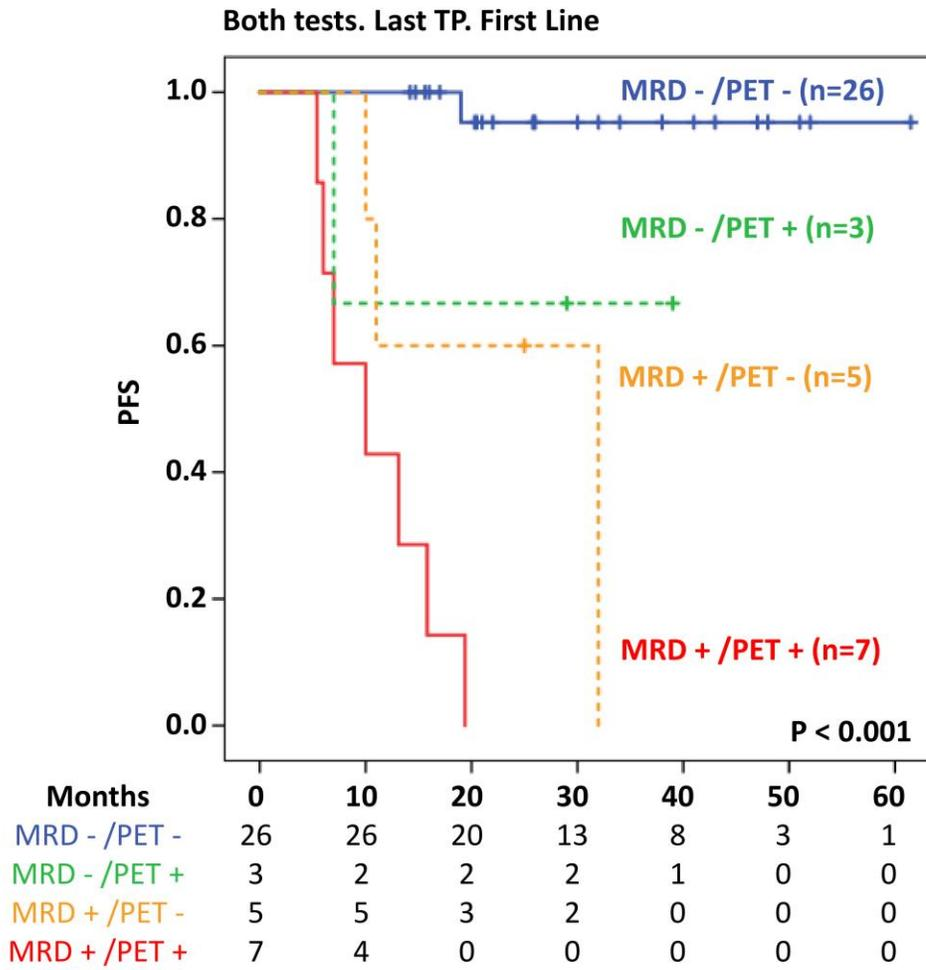
B. PET/CT Final (EOT). First line



655

656

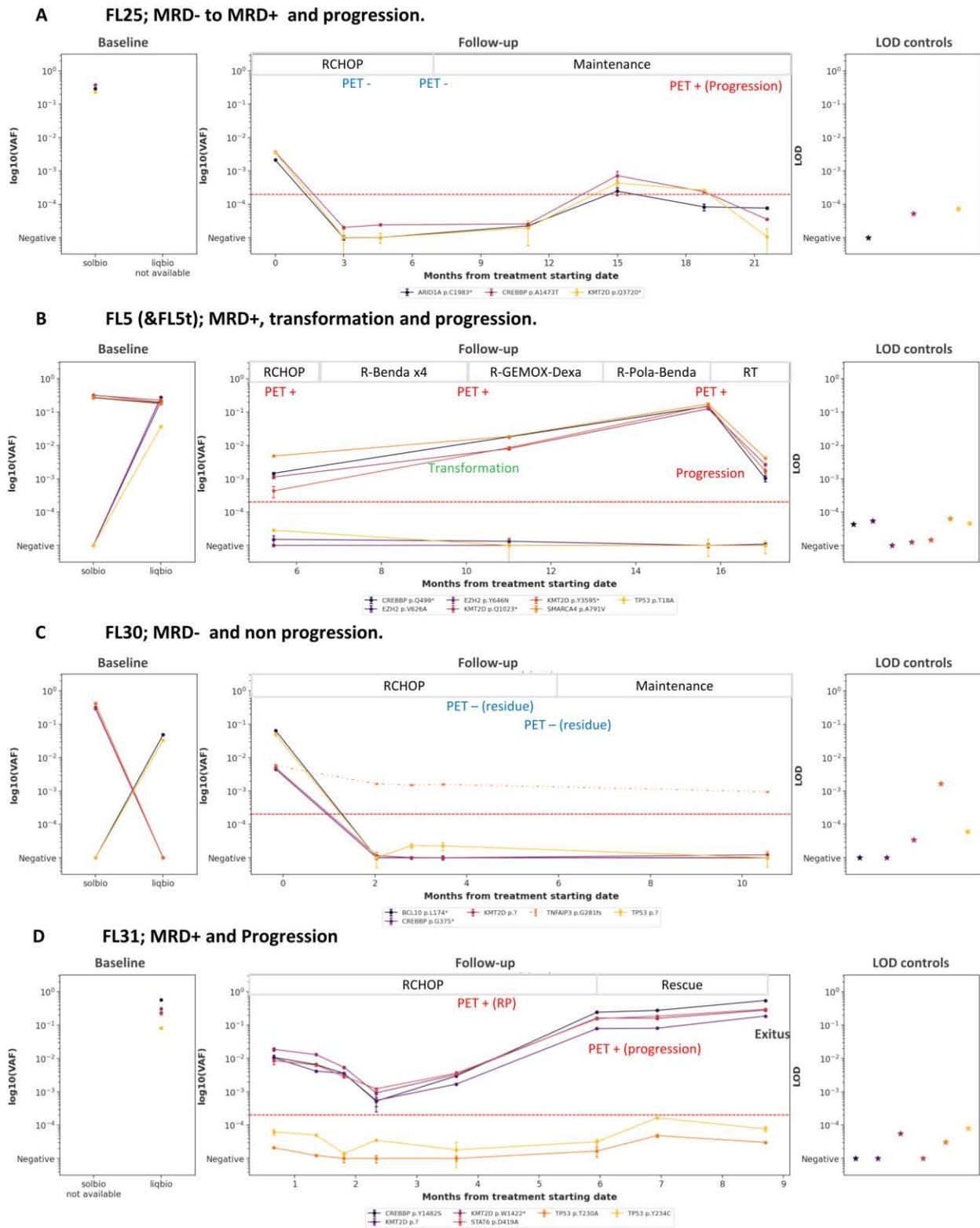
Figure 4



657

658

Figure 5



659